



**HAL**  
open science

## Receding Horizon Based Offline Gain Adjustment for Contour Error Reduction in High Speed Milling

Tan-Quang Duong, Pedro Rodriguez-Ayerbe, Sylvain Lavernhe, Christophe  
Tournier, Didier Dumur

► **To cite this version:**

Tan-Quang Duong, Pedro Rodriguez-Ayerbe, Sylvain Lavernhe, Christophe Tournier, Didier Dumur.  
Receding Horizon Based Offline Gain Adjustment for Contour Error Reduction in High Speed Milling.  
CIRP ICME '16 - 10th CIRP Conference on Intelligent Computation In Manufacturing Engineering,  
2016, Ischia, Italy. pp.227-232, 10.1016/j.procir.2016.06.040 . hal-02120164v2

**HAL Id: hal-02120164**

**<https://centralesupelec.hal.science/hal-02120164v2>**

Submitted on 10 Mar 2020

**HAL** is a multi-disciplinary open access archive for the deposit and dissemination of scientific research documents, whether they are published or not. The documents may come from teaching and research institutions in France or abroad, or from public or private research centers.

L'archive ouverte pluridisciplinaire **HAL**, est destinée au dépôt et à la diffusion de documents scientifiques de niveau recherche, publiés ou non, émanant des établissements d'enseignement et de recherche français ou étrangers, des laboratoires publics ou privés.

10th CIRP Conference on Intelligent Computation in Manufacturing Engineering - CIRP ICME '16

## Receding Horizon Based Offline Gain Adjustment For Contour Error Reduction In High Speed Milling

Tan-Quang Duong<sup>a,b,\*</sup>, Pedro Rodriguez-Ayerbe<sup>a</sup>, Sylvain Lavernhe<sup>b</sup>, Christophe Tournier<sup>b</sup>,  
Didier Dumur<sup>a</sup>

<sup>a</sup>L2S, CentraleSupélec - CNRS - Univ. Paris-Sud, Université Paris-Saclay, 91190 Gif-sur-Yvette, France

<sup>b</sup>LURPA, ENS Cachan, Univ. Paris-Sud, Université Paris-Saclay, 94235 Cachan, France

\* Corresponding author. Tel.: +33-781-615-767; fax: +33-169-851-389. E-mail address: [tanquang.duong@centralesupelec.fr](mailto:tanquang.duong@centralesupelec.fr)

### Abstract

Contour error rather than tracking error is the main concern in multi-axis machining with industrial High Speed Machines. Obtaining high contour performance using fixed gain controllers is not an easy task, especially in the case of complex forms having different curvature segments and different local feedrates along their profile. To tackle the problem, this paper presents an offline gain adjustment method based on a receding horizon window strategy to improve the accuracy of the machined contour. The prediction is performed using a nonlinear model of the machine tool axes. The conducted simulations show the efficiency of such an approach.

© 2016 The Authors. Published by Elsevier B.V.

Selection and peer-review under responsibility of the International Scientific Committee of "10th CIRP ICME Conference".

*Keywords:* Milling; Adaptive control; Gain adjustment

### 1. Introduction

Machining centers take an important place in the industrial manufacturing. An increasing demand for its accuracy and productivity requires the improvements both in mechatronic structure and in control strategies. While much success has been recorded for the former requirement, the later still has open doors for researchers.

Contour error (CE) is usually a crucial ruler for the accuracy of machined part in High Speed Machining (HSM). It refers to the shortest distance between the actual position and the desired contour of the tool path. Decreasing CE magnitude is therefore a privileged mission of contouring control.

To do such a control, Altintas et al. [1] proposed a sliding mode controller to reduce tracking error of each axis in yielding the CE reduction with the presence of changing friction, external disturbances and uncertainties in the drive inertia. However, the CE may be unfortunately increased due to the tracking error reduction that has been argued by Koren et al. [2]. Focusing on high contour performance, the authors

in [2,3] suggested that the contouring controller should take into account the coupling effect of the machine axes. Concerning this strategy, one trend is to build advanced controllers using feedbacks from coupled axes during the machining operation. Another is to use the coupling effect in simulation environment for pre-compensating the CE in machining process.

In the first coupling strategy, Zhang et al. [4] proposed a parametric predictive and variable universe fuzzy control method to guarantee the minimum CE. Meanwhile, Ghaffari et al. [5] used a modified position feedback to estimate the CE components that are then fed to the integral sliding mode control for position control of each axis. Besides, Model Predictive Control (MPC) has been successfully implemented in this control approach. Tang et al. [6] has integrated the CE and tracking error into the cost function of MPC and adjusted the feedrate adaptively to achieve the CE reduction. In addition, Lam et al. [7] has also developed a model predictive contouring control, where the weights in the cost function can be used to explicitly address the competing control objectives of minimizing CE as well as maximizing path speed.

In the second coupling strategy, Tounsi et al. [8] proposed an algorithm combining the constraints of cutting force magnitude, feedrate boundaries, changes in cutting geometry, contour error and feed drive dynamic to obtain the modified trajectory with optimized feedrate profile and pre-compensation of CE. Furthermore, modifying position setpoints by prediction models was also one of the potential solutions. Huo et al. [9] used two pre-trained nonlinear autoregressive networks with exogenous inputs, one for each axis, to predict the output position and the corresponding CE at the next sampling time. Yang et al. [10] implemented a MPC framework to obtain the same purpose, in which the reference position command is adjusted in considering the velocity and acceleration constraints of the machine axes.

The fact is that the commercial machining centers are usually offered in a built-in structure for users. Thus, it is difficult to implement the first coupling control strategy. More suitable solution is the second one, where many works were dedicated to modify the position setpoints in pre-compensating the CE. To the best of the authors' knowledge, there are rarely efforts in generating offline a set of variable gains in order to reduce the CE during the machining process. It is more interesting to note that these variable gains could be easily embedded in industrial HSM. Hence, a receding horizon based Offline Gain Adjustment (OGA) method is implemented in this paper to create such a set of variable gains.

The remainder of the paper is organized as follows. Section 2 presents the problem formulation, followed in Section 3 by the detailed explanation of the proposed OGA method. Then, the simulation results are discussed in Section 4. Finally, the paper is concluded in Section 5.

## 2. Problem formulation

In Fig. 1.a, classical definitions of biaxial control, e.g. in XZ plane, using fixed gain controllers are illustrated. At  $k^{\text{th}}$  instant,  $P_{d,k}$  and  $P_{a,k}$  are the desired and actual positions of the tool path respectively;  $E_{X,k}$  and  $E_{Z,k}$  are in turn the tracking errors of X and Z axes;  $E_k$  and  $\varepsilon_k$  are namely the norm of tracking error and the CE;  $t_{d,k}$  and  $t_{a,k}$  are the displacement vectors at the desired and actual positions respectively, with  $t_{d,k} = P_{d,k+1} - P_{d,k}$  and  $t_{a,k} = P_{a,k+1} - P_{a,k}$ . The desired contour represents the continuous trajectory to be followed by the axes associated to the setpoints generated by tool path interpolation. It usually differs from the actual one by the CE.

A general case of contouring control is shown in Fig. 1.b. At  $k^{\text{th}}$  instant, the cutting tool is at  $P_{a,k}$ , having the CE  $\varepsilon_k$ . Assume that within the dynamic capacity of the drive,  $C$  is the area that the cutting tool can reach. One can note that depending on the amplitude and direction of  $t_{a,k}$ , the CE may be increased or decreased in the next instant. In other words, the actual tool path may be closer or farther to the desired one at each instant, depending on the value of the displacement vector at the previous instant. Meanwhile, one of the factors affecting the vector  $t_{a,k}$  is the ratio of control gains on both axes. It means that if the control gains can be adjusted at each instant to obtain their optimal ratio that produces the optimal

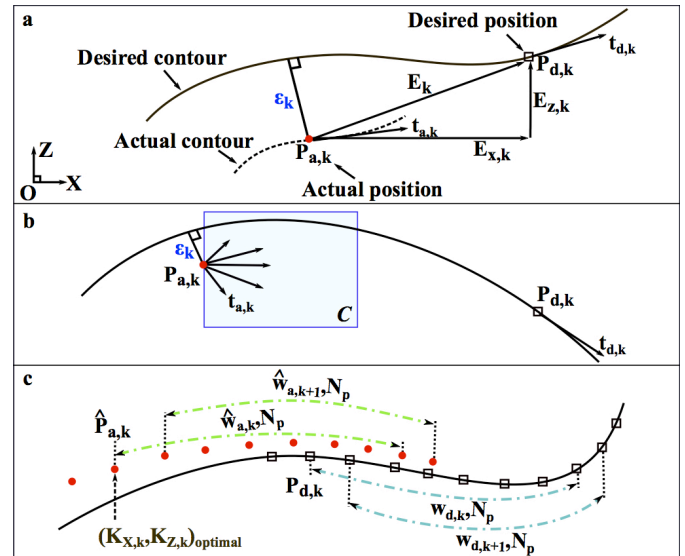


Fig.1. Relationship between CE and variable control gains

vector of displacement, the improvement in contour performance can be achieved.

Actually, the fixed gain controller cannot adjust its control gains to generate the optimal displacement vectors all over the trajectory to be machined. Thus, the contour performance in this kind of controller is not usually high. To overcome this weakness, the proposed idea is to build a contouring controller containing a set of variable control gains that can yield the optimal vectors of cutting displacement in the purpose of CE reduction. Moreover, to easily implement into the industrial HSM, the variable control gains should be generated by an offline algorithm before the machining process happens.

To realize this perspective, one of the feasible solutions is to use the idea of receding horizon in MPC, as shown in Fig. 1.c. The  $k^{\text{th}}$  control gains are selected by solving an optimization problem, which is to follow the setpoints  $P_{d,k}$  within the window  $w_{d,k}$  so that it produces the predicted positions  $\hat{P}_{a,k}$  having the minimum predicted CEs within the prediction window  $\hat{w}_{a,k}$ . The length of these windows is equal to  $N_p$ , so-called prediction horizon. After choosing the optimal control gains  $K_{X,k}$  and  $K_{Z,k}$ , the windows are receded to the next instant and the algorithm is repeated.

While the control gains could be adjusted by the receding horizon based optimization mechanism, its amplitude and variation frequency should be taken into account. The reason for this is that the corresponding axis behaviors should respect the kinematic constraints, including the velocity, acceleration and especially jerk. Moreover, the stability of the drive system is also a critical constraint.

Based on the above arguments, the detailed development of the receding horizon based OGA method is given in the following section.

## 3. Receding horizon based OGA method

Before developing the receding horizon based OGA method, the following important preparations should be executed firstly.

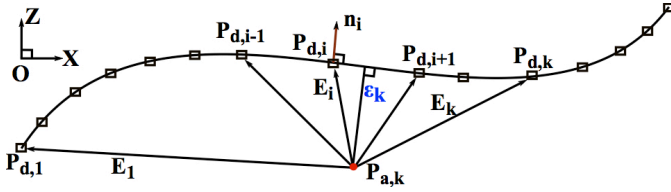


Fig. 2. CE model

Table 1. Kinematic characteristics of Mikron machine.

	$V_{max}$ (m/min)	$A_{max}$ (m/s <sup>2</sup> )	$J_{max}$ (m/s <sup>3</sup> )
X axis	30	2.5	10
Z axis	30	2.1	100

### 3.1. Kinematic constraints and setpoints generation

To avoid the vibration in the machine tool, the kinematic constraints of the axes should be respected. In this paper, the case study is a biaxial contouring control of the 5-axis Mikron UCP 710 machining center, where the velocity, acceleration and jerk limits of the concerned axes are given in Table 1.

Considering the above constraints, the position setpoints are generated from the reference tool path by a feed-planning algorithm that allows producing a smooth movement. To well handle this scheme, the Velocity Profile Optimization (VPOp) algorithm proposed in [11] is used. This approach can be applied to any articulated mechanical structure.

### 3.2. CE calculation model

In contour following, authors usually add the CE into the cost function to formulate the optimization problem. Thus, the more accurate CE calculation, the more efficient contouring controller. In the offline execution, the CE can be calculated by the line interpolation based CE model [12]. In Fig. 2, the CE  $\epsilon_k$  is computed by the following two steps:

- At  $k^{th}$  instant of the simulated machining, determine the closest desired position  $P_{d,i}$  to the point  $P_{a,k}$ , with  $i = 1:k$ . The point  $P_{d,i}$  is characterized by the vector  $E_i$  and the normal vector  $n_i$ .
- The CE, which is the shortest distance from  $P_{a,k}$  to the previous and next segments of  $P_{d,i}$ , is calculated by (1).

$$\epsilon_k = \text{sign}(\overline{n_i} \cdot \overline{E_i}) \frac{|\overline{P_{d,i}P_{d,i+1}} \times \overline{P_{d,i}P_{a,k}}|}{|\overline{P_{d,i}P_{d,i+1}}|} \quad (1)$$

### 3.3. Nonlinear axis model

Traditionally, the machine tool axis is controlled by a cascade control structure. Fig. 3 illustrates this structure for the Z axis for example, with the specificity that the proportional gain  $K_{pz}$  (m/min/mm) is now a set of variable values generated by OGA. The external position loop is controlled by a proportional controller combined with a feed forward (FFW) action, while it is internally controlled respectively by speed and current PI controllers in velocity and current loops [13]. Note that for simplicity purposes, the current loop and the motor are hidden. From this framework,

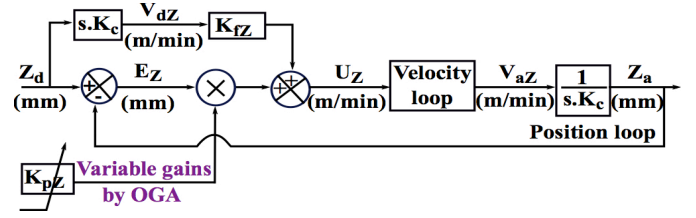


Fig. 3. Cascade control structure for Z axis

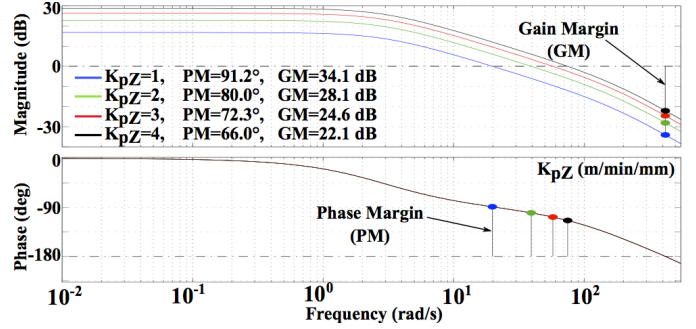


Fig. 4. Bode diagram for position open loop of Z axis

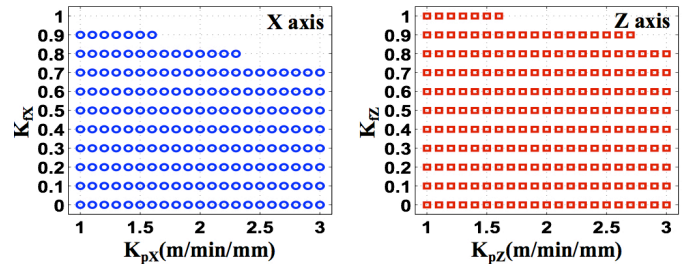


Fig. 5. Gain tuning satisfying the kinematic constraints

the desired and actual positions are namely denoted by  $Z_d$  and  $Z_a$ , while  $E_z = Z_d - Z_a$  is the tracking error;  $K_c$  and  $K_{fz}$  are in turn the conversion factor from mm/s to m/min and the FFW gain. The inertia and the nonlinear characteristics of the axis due to frictions identified in [14] are used to simulate the behavior of the real machine tool axis.

### 3.4. Gain range defined by stability criterion

From Fig. 3, the stability criterion of the position loop consists in analyzing the Phase Margin (PM) and Gain Margin (GM) of the position open loop, which should usually be greater than 70° and 10 dB, respectively. The bode diagram for the position open loop, which is linearized from the nonlinear axis model in Section 3.3, is used to evaluate the PM and GM of different  $K_p$  values. Fig. 4 illustrates that of Z axis for example. This gain tuning allows obtaining the stabilized gain ranges of  $K_p$  for both axes as [1:3] (m/min/mm). Meanwhile, the  $K_f$  being outside the loop does not deteriorate the system stability and is usually tuned in the range of [0:1].

### 3.5. Gain range defined by kinematic constraints

Another gain tuning is performed in considering the kinematic constraints in Table 1, in which the actual velocity, acceleration and jerk of each machine axis at  $k^{th}$  instant are

limited respectively as  $0 \leq |v_{a,k}| \leq V_{\max}$ ,  $0 \leq |a_{a,k}| \leq A_{\max}$ ,  $0 \leq |j_{a,k}| \leq J_{\max}$ . Let  $S_{a,k}$  denote for the position of each axis  $\{X_{a,k}, Z_{a,k}\}$  and  $T_e$  is the sampling time, having

$$\begin{cases} \Delta S_{a,k} = S_{a,k+1} - S_{a,k} \\ v_{a,k} = \Delta S_{a,k} / T_e \\ a_{a,k} = (v_{a,k} - v_{a,k-1}) / T_e \\ j_{a,k} = (a_{a,k} - a_{a,k-1}) / T_e \end{cases}$$

The kinematic constraints are rewritten as:

$$\begin{cases} 0 \leq |\Delta S_{a,k} / T_e| \leq V_{\max} \\ 0 \leq |(\Delta S_{a,k} - \Delta S_{a,k-1}) / T_e^2| \leq A_{\max} \\ 0 \leq |(\Delta S_{a,k} - 2\Delta S_{a,k-1} + \Delta S_{a,k-2}) / T_e^3| \leq J_{\max} \end{cases} \quad (2)$$

The tuning based on the stabilized gain ranges in section 3.4 is now to find the combination of the control gains  $K_p$  and  $K_f$  so that (2) is satisfied all over the machining operation. Moreover, to remain with a reasonable computation load, both  $K_p$  and  $K_f$  are tuned with the gain steps of 0.1. In fact, one value of  $K_p$  combined with one value of  $K_f$  forms one control configuration for the position loop in Fig. 3. By verifying the axis behaviors simulated with the position closed loop, Fig. 5 shows that there are 189 (blue circles) and 214 (red squares) gain configurations for X and Z axes, respectively.

### 3.6. Principle of the receding horizon based OGA method

Generally, the proposed OGA method is inspired from the idea of MPC, but it only takes two excellent features of this technique including the receding horizon and the constraints in control inputs. According to the analysis in Section 2 and the control structure in Fig. 3, let  $N_p$  represents the prediction horizon. At the  $k^{th}$  instant, denoting:

$$\begin{cases} K_{p,k} = [K_{pX,k}, K_{pZ,k}]^T \\ \mathcal{P}_{d,k} = [P_{d,k}, P_{d,k+1}, \dots, P_{d,k+N_p-1}]^T \\ \hat{\mathcal{P}}_{a,k} = [\hat{P}_{a,k}, \hat{P}_{a,k+1}, \dots, \hat{P}_{a,k+N_p-1}]^T \end{cases} \quad (3)$$

where  $K_{p,k}$  is the optimized proportional gain vector;  $P_{d,j} = [X_{d,j}, Z_{d,j}]$ ,  $\hat{P}_{a,j} = [\hat{X}_{a,j}, \hat{Z}_{a,j}]$ , with  $j = k : k + N_p - 1$ , are respectively the desired and predicted position vectors within the prediction horizon.

From  $\mathcal{P}_{d,k}$  and  $\hat{\mathcal{P}}_{a,k}$  in (3), the predicted contour error  $\hat{\mathcal{E}}_k$  can be computed by (1) and presented as:

$$\hat{\mathcal{E}}_k = [\hat{\mathcal{E}}_k, \hat{\mathcal{E}}_{k+1}, \dots, \hat{\mathcal{E}}_{k+N_p-1}]^T \quad (4)$$

The cost function is defined in a quadratic form as:

$$\mathcal{J}_k = \hat{\mathcal{E}}_k^T \hat{\mathcal{E}}_k + \lambda \Delta K_{p,k}^T \Delta K_{p,k} \quad (5)$$

in which  $\Delta K_{p,k} = K_{p,k} - K_{p,k-1}$  is the increment of the proportional gain;  $\lambda$  is a weigh factor allowing to tune the behavior of the gain increment, i.e. high  $\lambda$  means that only small gain increment will be acceptable.

According to the analysis in Section 3.4, the  $K_{p,k}$  should be optimized in the stabilized gain range, so

$$K_{stabilized, \min} \leq K_{p,k} \leq K_{stabilized, \max} \quad (6)$$

Therefore,

$$K_{stabilized, \min} - K_{p,k-1} \leq \Delta K_{p,k} \leq K_{stabilized, \max} - K_{p,k-1} \quad (7)$$

In addition, the cost function in (5) is also subject to the axis kinematic constraints defined by (2), in which  $\Delta S_{a,k-1}$  and  $\Delta S_{a,k-2}$  have been stored in the previous instants, the boundaries of axes displacement and velocity at  $k^{th}$  instant can be found as:

$$\begin{cases} \Delta S_{k, \min} \leq \Delta S_{a,k} \leq \Delta S_{k, \max} \\ \Delta S_{k, \min} / T_e \leq v_{a,k} \leq \Delta S_{k, \max} / T_e \end{cases} \quad (8)$$

where  $S_{a,k}$  can be written by a vector form as  $[X_{a,k}, Z_{a,k}]^T$  and  $v_{a,k} = [V_{aX,k}, V_{aZ,k}]^T$ .

Supposing the transfer function of velocity loop in Fig. 3 is equal to 1, its velocity setpoint is calculated by:

$$\begin{cases} u_k = E_k (K_{p,k-1} + \Delta K_{p,k}) + V_{d,k} K_f \\ u_k = v_{a,k} \end{cases} \quad (9)$$

in which,

$$\begin{cases} u_k = [U_{X,k}, U_{Z,k}]^T \\ K_f = [K_{fX}, K_{fZ}]^T \\ V_{d,k} = \text{diag}(V_{dX,k}, V_{dZ,k}) \\ E_k = \text{diag}(E_{X,k}, E_{Z,k}) \end{cases}$$

From (8) and (9), the limits of gain increment are found as:

$$(\Delta K_{p,k})_{\min} \leq \Delta K_{p,k} \leq (\Delta K_{p,k})_{\max} \quad (10)$$

where the limits of  $\Delta K_{pZ,k}$  for example are given as:

$$\Delta K_{pZ,k, \min, \max} = \frac{1}{E_{Z,k}} \left( \frac{\Delta Z_{k, \min, \max}}{T_e} - V_{dZ,k} K_{fZ} \right) - K_{pZ,k-1}$$

Consequently, if  $\Delta K_{p,k}$  satisfies (10), the kinematic constraints in (2) are respected also. Hence, the problem is to minimize  $\mathcal{J}_k$  in (5), being subject to the constraint of gain increment in (7) and (10).

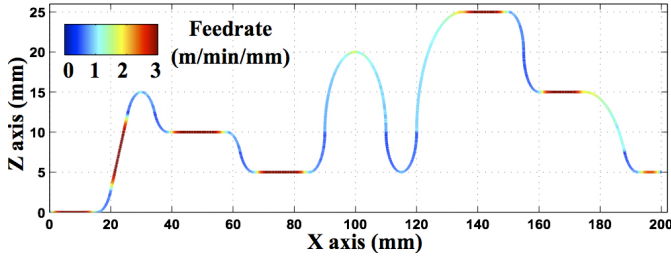


Fig. 6. Position setpoint generation

Table 2. Control gain configuration.

	C1	C2
$K_{pX}$ (m/min/mm)	1.6	1.6
$K_{fX}$	0.9	0.9
$K_{pZ}$ (m/min/mm)	1.6	[1:2.7]
$K_{fZ}$	0.9	0.9

Because there is a large number of  $\Delta K_{p,k}$  that can be tuned to satisfy (6) and (9), this leads to a burden of computation time in the optimization problem. It makes sense that a trade-off between the optimal  $\Delta K_{p,k}$  value and the computation time should be considered.

To summarize, the OGA performs the following steps at the  $k^{th}$  instant:

- Step 1: Initialize  $N_p$  and  $\lambda$ .
- Step 2: Calculate the gain increment limits in (7) and (10).
- Step 3: Tune the gain increment  $\Delta K_{p,k}$  satisfying Step 2. Each value of  $\Delta K_{p,k}$  defines one cost function  $\mathcal{J}_k$  in (5).
- Step 4: Choose the optimized  $\Delta K_{p,k}$  in Step 3 that obtains the minimum  $\mathcal{J}_k$ .
- Step 5: The optimized  $K_{p,k}$  corresponding with the optimized  $\Delta K_{p,k}$  in Step 4 is applied to  $k^{th}$  instant and then the OGA is receded to the  $(k+1)^{th}$  instant.

#### 4. Results

Firstly, the position setpoints generated by VPOp algorithm [11] are shown in Fig. 6, with a programmed feedrate of 3 (m/min), interpolation tolerance of  $20 \mu m$  and the sampling time  $T_e = 1 ms$ .

To prove the efficiency of the proposed OGA algorithm, the following two cases of study are conducted:

- For both axes,  $K_p$  and  $K_f$  are fixed in the position loop. (C1)
- For X axis,  $K_{pX}$  and  $K_{fX}$  is kept fixed. For Z axis,  $K_{fZ}$  is fixed, while  $K_{pZ}$  is adjusted by OGA. (C2)

In table 2, according to the gain range in Section 3.4 and Section 3.5, the best fixed gains for C1 are chosen so that the minimum mean square of contour error, MSE(CE), is obtained. The fixed gains and the adjustment gain range for C2 are also chosen. In fact, the OGA can be applied for both axes and for adjusting  $K_p$  and/or  $K_f$ , but due to the simulation purpose and the computation burden, only the case C2 is taken into the case study.

Accepting the trade-off between the optimal value and computation burden,  $\Delta K_{p,k}$  is tuned in the following range:  $\Delta K_{p,k} = [\alpha_2 \Delta K_{min}, \alpha_1 \Delta K_{min}, 0, \alpha_1 \Delta K_{max}, \alpha_2 \Delta K_{max}]$ , with  $\alpha_1 = 0.01$ ,  $\alpha_2 = 0.05$ ;  $\Delta K_{min}$  and  $\Delta K_{max}$  are calculated at each instant by (7) and (10).

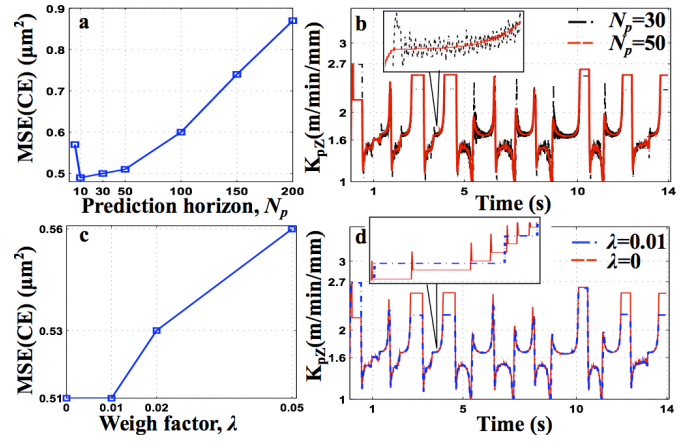


Fig. 7. Tuning  $N_p$  with  $\lambda = 0$  (a, b) Tuning  $\lambda$  with  $N_p = 50$  (c, d)

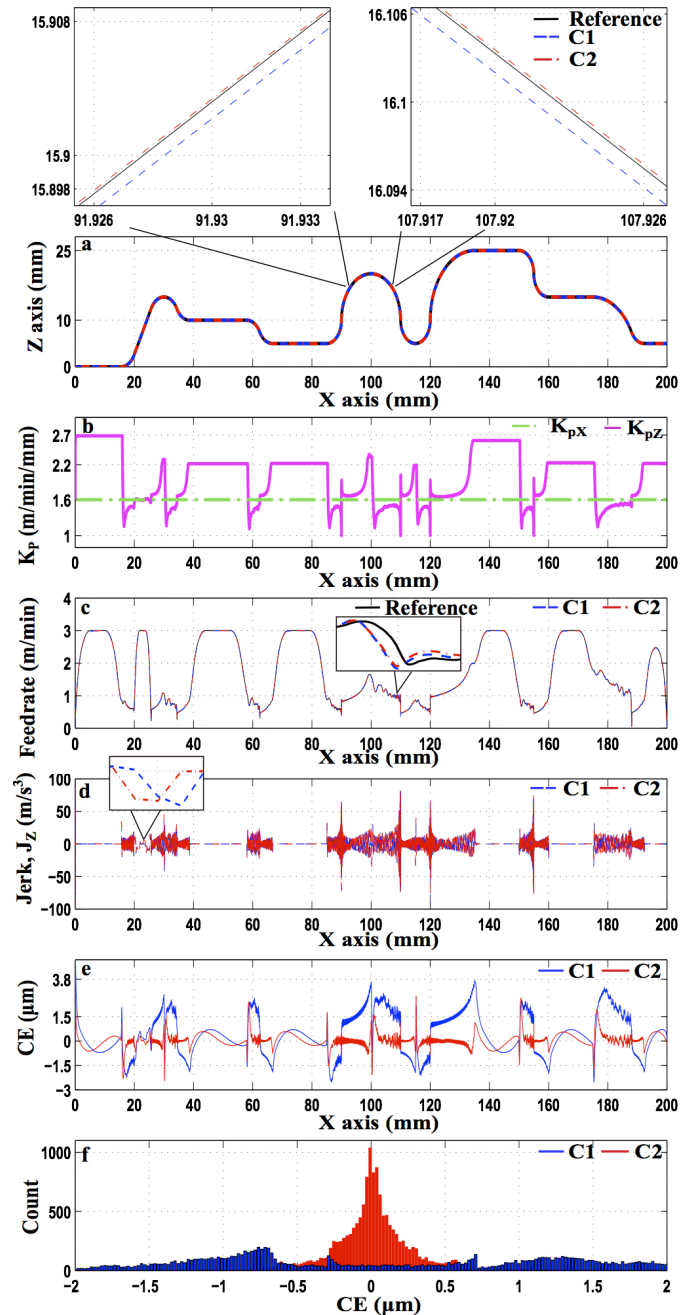


Fig. 8. Effects of adjusted variable gains in the geometry domain

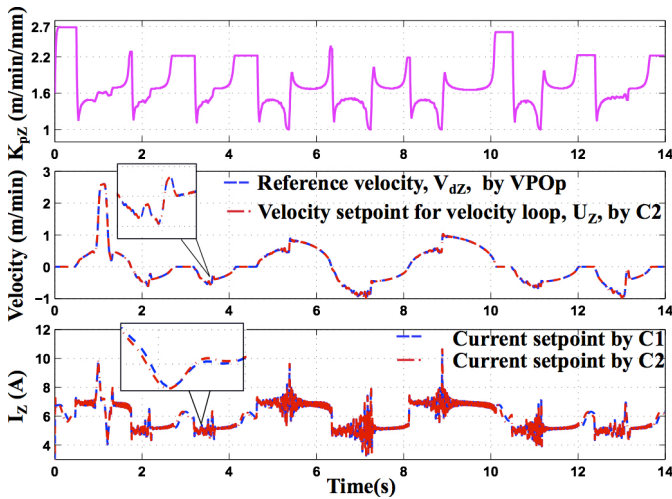


Fig. 9. Effect of adjusted variable gains in the time domain

Table 3. Contouring performance.

	C1	C2
MSE(CE) ( $\mu m^2$ )	2.26	0.51
Improvement	Reference	77.43 %

In Fig. 7.a and Fig. 7.b, the prediction horizon  $N_p$  is tuned while the weigh factor is kept fixed as  $\lambda = 0$ . It can be seen that  $N_p = 50$  can provide the small MSE(CE) and the relatively smooth variable gains. Using this prediction horizon, the tuning of weigh factor is shown in Fig. 7.c and Fig. 7.d, where it illustrates the effects of weigh factor on the contour performance and the variable gain behavior. With  $\lambda = 0.01$ , the small peaks in gain increment with  $\lambda = 0$  is rejected, while the MSE(CE) is the same for both cases. Therefore,  $N_p = 50$  and  $\lambda = 0.01$  is chosen for C2.

Using these configurations, the simulated contour in machining with C2 is closer to the reference trajectory than that with C1, as shown in Fig. 8.a. The selected variable gains  $K_{pz}$  generated by OGA are illustrated in Fig. 8.b. As can be observed there is a correlation between the change of  $K_{pz}$  and the change of curvature. From Fig. 8.c and Fig. 8.d, the feedrate and the jerk of Z axis in both cases respect the constraints in Table 1.

Meanwhile, Fig. 8.e represents the CE behavior in both cases. In the case of C1, the CE at curved segments is bigger than that at straight lines. When the segment changes from convex to concave curves, the CE changes its sign. In contrast, the CE at curved segments of C2 has been remarkably reduced. In Fig. 8.f, the CE in C2 has a centered normal distribution, ranging from  $-0.5$  to  $0.5 \mu m$ , while C1 induces the CE mainly between  $0.5$  and  $2 \mu m$  on both sides of the desired contour.

Furthermore, the behavior and effect of the variable gains  $K_{pz}$  produced by OGA has been also examined in the time domain in Fig. 9. It can be said that the variable proportional gains of Z axis do not deteriorate the velocity setpoints derived from the control actions of position loop and the current setpoints derived from the speed PI controller. In the quantitative point of view, the MSE(CE) in C2 has been reduced by about three fourth of that in C1, as seen in Table 3.

## 5. Conclusion

In the purpose of generating offline the variable gains along the trajectory for pre-compensating the CE in the machining operation, the receding horizon based OGA method has been developed. This approach offers the prediction functionality for the contouring controller. From the above results, it can be concluded that the proposed OGA method leads to a significant improvement in contouring performance, as comparing to the traditional fixed gain controller, while all of the kinematic constraints and stability criterion are also maintained satisfied. Only the proportional gain of Z axis is adjusted by OGA in the current case study, the application of OGA for other axes of machine tool will be a part of future work.

## Acknowledgements

This work, N° 2014-812D – Projet OMEGA, is supported by DIGITEO foundation.

## References

- [1] Altintas Y, Erkorkmaz K, Zhu W H. Sliding mode controller design for high speed feed drives. CIRP Annals – Manuf Techno; vol. 49, no. 1, pp. 265–270, 2000.
- [2] Koren Y, Lo C C. Variable-gain cross-coupling controller for contouring. CIRP Annals – Manuf Techno; vol. 40, no. 1, pp. 371–374, 1991.
- [3] Chiu G-C, Tomizuka M. Contouring control of machine tool feed drive systems: a task coordinate frame approach. IEEE Trans on Control Syst Techno; vol. 9, no. 1, pp. 130–139, January 2001.
- [4] Zhang L, Wu T, Huang F. A coupling motional control method based on parametric predictive and variable universe fuzzy control for multi-axis cnc machine tools. Int J Adv Manuf Technol; September 2014.
- [5] Ghaffari A, Ulsoy A. Dynamic contour error estimation and feedback modification for high-precision contouring. IEEE/ASME Trans on Mechatronics; vol. PP, no. 99, pp. 1–1, 2015.
- [6] Tang L, Landers R G. Predictive contour control with adaptive feed rate. IEEE/ASME Trans on Mechatronics; vol. 17, no. 4, pp. 669–679, Aug 2012.
- [7] Lam D, Manzie C, Good M C. Model predictive contouring control for biaxial systems. IEEE Trans on Control Syst Techno; vol. 21, no. 2, pp. 552–559, March 2013.
- [8] Tounsi N, Elbestawi M. Optimized feed scheduling in three axes machining. part I: Fundamentals of the optimized feed scheduling strategy. Int J of Mach Tools and Manuf; vol. 43, no. 3, pp. 253–267, 2003.
- [9] Huo F, Poo A N. Nonlinear autoregressive network with exogenous inputs based contour error reduction in CNC machines. Int J of Mach Tools and Manuf; vol. 67, pp. 45–52, 2013.
- [10] Yang S, Ghasemi A H, Lu X, Okwudire C E. Precompensation of servo contour errors using a model predictive control framework. Int J of Mach Tools and Manuf; vol. 98, pp. 50–60, 2015.
- [11] Beudaert X, Lavernhe S, Tournier C. Feedrate interpolation with axis jerk constraints on 5-axis nurbs and g1 tool path. Int J of Mach Tools and Manuf; vol. 57, pp. 73–82, June 2012.
- [12] Zhao G, An H, Zhao Q. Contour error coupled-control strategy based on line interpolation and curve interpolation. J of Computer; vol 8, no. 6, pp. 1512–1519, June 2013.
- [13] Rodriguez-Ayerbe P, Dumur D, Lavernhe S. Axis control using model predictive control: identification and friction effect reduction. 3rd Int Conf on Virtual Machi Process Tech; p. 8, May 2014.
- [14] Prévost D, Lavernhe S, Lartigue C, and Dumur D. Feed drive modelling for the simulation of tool path tracking in multi-axis high speed machining. Int J of Mechatronics and Manuf Sys; vol. 4, no. 3–4, pp. 266–284, January 2011.